

Data Analysis Of Near Vertical Incidence Skywave (NVIS) Propagation In Pekanbaru

Sutoyo
Electrical Engineering
Department,
Universitas Islam Negeri Sultan
Syarif Kasim Riau
Pekanbaru, Indonesia
sutoyo@uin-suska.ac.id

Dony Hendra
Electrical Engineering
Department,
Universitas Islam Negeri Sultan
Syarif Kasim Riau
Pekanbaru, Indonesia
Dony_hk27@yahoo.com

Varulintor Dear,
Badan Riset Inovasi Nasional
(BRIN)
Bandung, Indonesia
varuliantor.dear@lapan.go.id.

Muhammad Isnaini Hadiyul
Umam
Industrial Engineering
Department,
Universitas Islam Negeri Sultan
Syarif Kasim Riau
Pekanbaru, Indonesia
muhammad.isnaini@uin-
suska.ac.id

Dedi Irawan
Physics Department,
PMIPA, FKIP Universitas Riau
Pekanbaru, Indonesia
dedi.irawan@lecturer.unri.ac.id

Muhammad Rizki
Industrial Engineering Department,
Universitas Islam Negeri Sultan Syarif
Kasim Riau
Pekanbaru, Indonesia
muhammad.rizki@uin-suska.ac.id

Muhammad Luthfi Hamzah
Information System Department,
Universitas Islam Negeri Sultan Syarif
Kasim Riau
Pekanbaru, Indonesia
muhammad.luthfi@uin-suska.ac.id

Abstract— Solar activity has a major influence on the condition of the ionosphere layer which causes the characteristics of the ionosphere layer to change every time. This will certainly have an impact on the success of HF radio communication which is very dependent on the ionosphere layer. One of the impacts of solar activity is the variation in the ionosphere layer which has an 11-year cycle phase causing changes in the value of foF2. This study aims to analyze the measurement data of the ionospheric layer (ionosonda) to see the effect of the half cycle of solar activity for the period 2010 to 2015 which can be used for the Pekanbaru area, Indonesia with Near Vertical Incidence Skywave (NVIS) propagation mode. The results of the study indicate that there are differences in the use of working frequencies for each year that can be used between 2 MHz to 10 MHz, with the right communication time at 08.00 UTC+7 to 22.00 UTC+7. The change in the highest frequency value is caused by positive storms and negative storms that occur in the ionosphere layer which will interfere with high frequency radio communications and satellite-based navigation

Keywords— Solar activity, NVIS, HF Radio, Ionosonda.

I. INTRODUCTION

Technology in the field of telecommunications continues to develop in supporting and providing educational activities, both in the form of means of using fiber optics [1][2][3], wireless communication[4][5][6] as well as using satellite communications[7][8][9][10][11]. In addition, the need for telecommunications is also needed in disaster emergencies to support information related to evacuation [12][13][14]. The technology that can be used for this condition is Radio HF (High Frequency) Radio Communication[15][16]. HF Radio Communication (High Frequency; 3-30 MHz) is one of the main solutions in disaster management mitigation. This is because HF radio communication has the advantage of being independent and able to reach long-distance communications.

The propagation of radio waves in the HF spectrum predominantly utilizes the ionosphere layer as a medium for propagation of radio waves and is known as space propagation (Skywave). Near Vertical Incidence Skywave (NVIS) propagation mode is a form of space propagation mode that has a short range communication coverage which is a combination of skywave and ground wave propagation [17][18][19][20][21].

The success of communication using space propagation (skywave) is strongly influenced by the condition of free electrons in the ionosphere layer. The free electrons in the ionosphere will remain separated from the atoms for a short period of time before being attracted and combined with positive ions due to the influence of electrostatic forces. The ionization process in the ionosphere is strongly influenced by solar activity. The dynamic condition of the ionospheric layer affects the working frequency range that can be used in a communication circuit. With the ionospheric observation data in the Kototabang area, Indonesia in the 2010-2015 period which represents the minimum phase, it can be used as material for analyzing the openness of NVIS mode radio communication channels in the Pekanbaru area. For now, monitoring the dynamic Ionosphere layer [22], and its influence on HF radio communication, has had a measurement station using Automatic Link Establishment (ALE) [23],[24], as well as using ionosonda radar [25][26].

II. METHODOLOGY

The following is a flow chart of the research starting from the data collection to the conclusion of the study. This research uses ionogram data from Kototabang ionosonda radar observations to see variations in the openness of HF radio communication channels based on the reflectivity of the ionospheric layer. Data from the ionosonda radar which represents the ionosphere conditions with a radius of 300 km above Kototabang can be used to represent the ionospheric

conditions above Pekanbaru. Scaling method based on URSI is used to process ionogram data into f_{min} , f_{oF2} , $h'f$ data

The following is a flowchart of the stages of ionogram data processing.

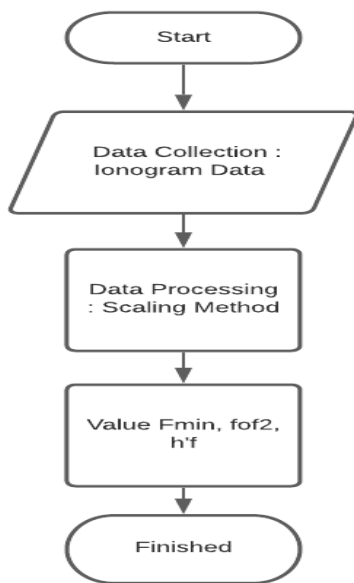


Fig. 1. Data Processing

The stages of the ionogram data processing process using the scaling method. The scaling method is used to convert ionogram data in the form of point codes into numerical parameters. The data parameters to be processed represent the minimum frequency (f_{min}), critical frequency (f_{oF2}) and layer height F ($h'f$) which are used as variables for the calculation of LUF, MUF and OWF.

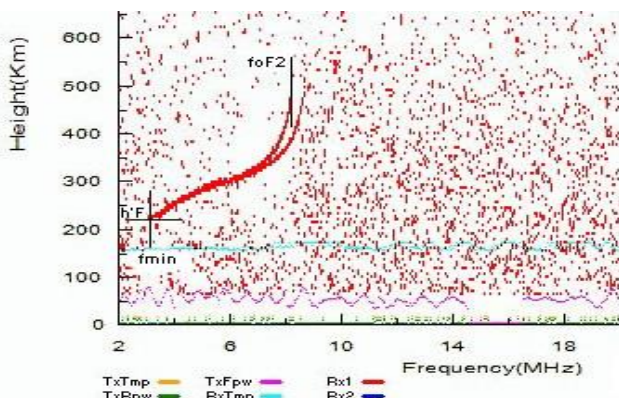


Fig. 2. Data ionogram

The picture above is about reading the values of f_{min} , f_{oF2} and $h'f$ it can be explained that :

1. The minimum frequency value (f_{min}) is the lowest frequency value in the F layer of the ionosphere.
2. The critical frequency value (f_{oF2}) is a value that represents the highest frequency in the F layer of the ionosphere. This characteristic value will reach its peak value during the day and vice versa occurs at night.

3. This characteristic value will reach its peak value during the day and vice versa occurs at night.

- a. Calculation of LUF, MUF and OWF

Calculation of the values of Lowest Usable Frequency (LUF), Maximum Usable Frequency (MUF) and Optimum Usable Frequency (OWF) is performed to obtain a frequency value that can be used as a reference for the working frequency of HF radio communications. Determination of the frequency value reflected by the ionosphere layer can be obtained from a simple calculation using the secant method. In the equation of the secant method it is stated that the determinants of the frequency value reflected by the ionosphere layer are; distance (d), critical frequency/vertical frequency (f_o/f_v), and altitude (h).

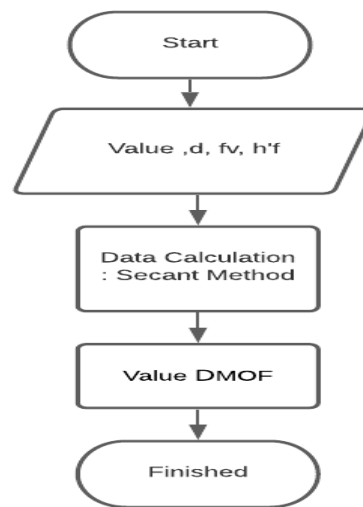


Fig. 3. Calculation of LUF, MUF and OWF

III. RESULT AND DISCUSSION

The results of data processing are presented in the form of information images in the form of the minimum frequency (f_{min}), the height of the ionosphere layer (h) and the critical frequency in the layer (f_{oF2}). From these parameters, calculations can be made to determine the lowest usable frequency (LUF) and maximum usable frequency (MUF). So from this value, the best working frequency range can be obtained, namely the optimum usable frequency (OWF).

A. Ionosonda Radar Observation Results

Data from observations of the condition of the ionosphere layer is called ionogram data. Ionogram data processing is done by determining the numerical value of the ionospheric parameter from the altitude graph as a function of frequency. This process is known as the scaling process. The scaling process follows the standard, namely the Undergraduate Research Summer Institute (URSI). The parameters of the ionospheric layer that can be obtained from the scaling process include the minimum frequency value (f_{min}), critical frequency (f_{oF2}) and the height of the ionosphere layer (h'). The results of ionosonda radar observations on 1 January , 2010 at 00.00 UTC+ 7, it is known that the value of f_{min} is at a frequency of 2 MHz, the

value of foF2 is at a frequency of 9.37 MHz and is located at an altitude of 236 km above the earth's surface. Based on the assumption that the distance between Pekanbaru and Kototabang has a distance of 189 Km, it can be calculated to get the lowest usable frequency (LUF), maximum usable frequency (MUF) and Optimum usable frequency (OWF) values using the Secant method as follows :

$$LUF = f_{min} \sqrt{\frac{\frac{1}{4}d^2 + h^2}{h}} \tag{1}$$

$$LUF = 2 \sqrt{\frac{\frac{1}{4}189^2 + 236^2}{236}}$$

$$LUF = 2 \sqrt{\frac{\frac{1}{4}35.721 + 55.696}{236}}$$

$$LUF = 2 \sqrt{\frac{64.626,25}{236}}$$

$$LUF = 2.154 \text{ MHz}$$

Meanwhile, to find the MUF value with the secant method as follows:

$$MUF = foF2 \sqrt{\frac{\frac{1}{4}d^2 + h^2}{h}} \tag{2}$$

$$MUF = 9,37 \sqrt{\frac{\frac{1}{4}189^2 + 236^2}{236}}$$

$$MUF = 9,37 \sqrt{\frac{\frac{1}{4}35.721 + 55.696}{236}}$$

$$MUF = 9,37 \sqrt{\frac{64.626,25}{236}}$$

$$MUF = 10 \text{ MHz}$$

So to determine the value of OWF = 0,85 x MUF

$$OWF = 0,85 \times 10,00 \text{ MHz}$$

$$OWF = 8.50 \text{ MHz}$$

From the results of the calculation of the values of fmin and foF2 using the Secant method, it is stated in the form of table 1.

TABLE 1. CALCULATION RESULTS VALUES OF LUF, MUF AND OWF.

Time (UTC+7)	LUF	OWF	MUF
00.00	2,2	8,5	10
01.00	2,1	7,7	9,1
02.00	2,2	7,4	8,7
03.00	2,2	6,1	7,2
04.00	2,1	4,6	5,4
05.00	2,1	4,1	4,9
06.00	2,1	4,3	5,0
07.00	2,1	6,2	7,3
08.00	2,2	7,8	9,2

09.00	2,2	8,3	9,8
10.00	2,2	7,2	8,5
11.00	2,2	7,6	8,9
12.00	2,2	9,9	11
13.00	4,3	12	13
14.00	3,1	9,5	11
15.00	3,0	6,8	8,0
16.00	2,2	7,3	8,6
17.00	2,3	10	11
18.00	2,1	9,4	11
19.00	2,1	8,5	10
20.00	2,1	7,7	9,1
21.00	2,1	8,0	9,4
22.00	2,1	8,2	9,6
23.00	2,1	7,8	9,2

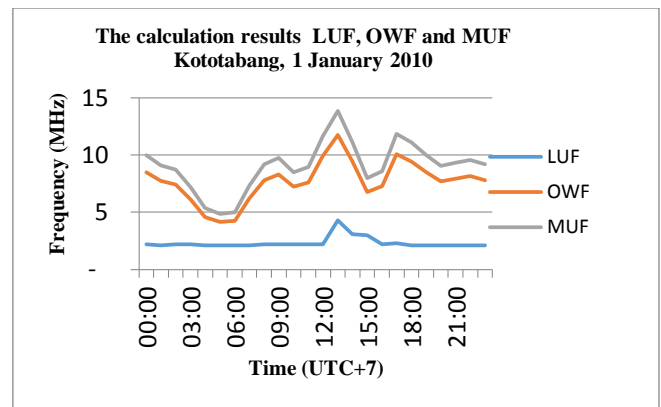


Fig. 4. Calculation Results of Daily Observation Data LUF, OWF and MUF.

Figure 4 is the result of the calculation of the LUF, OWF and MUF values showing that the LUF and MUF frequencies have variations every time. The difference in frequency at any time is influenced by solar activity in emitting x-rays and Extreme Ultra Violet (UEV) rays in the ionosphere layer. Nilai LUF dan MUF tends to be constant at its lowest position at night and will rise during the day following the intensity of the sun. The lowest LUF value on the graph is at a frequency of 2.1 MHz at 01.00 UTC+7 and at 13.00 UTC+7 the LUF value increases at a frequency of 4.3 MHz. Meanwhile, the lowest MUF value is at 05.00 UTC+7 on the 5 MHz frequency and at 13.00 UTC+7 the MUF value has increased at 13.9 MHz frequency.

B. Analysis of Variations in the Openness of HF Radio Communication Channels

Based on the results of observations of the ionospheric layer that have been carried out using the Kototabang ionosonda radar in 2010 to 2015 which represents a half cycle of solar activity, it can be used to determine variations in the openness of HF radio communication channels and can be seen the effects caused by solar activity. The results of the calculation are LUF, MUF and OWF values which represent the limit of working frequency for one day of observation. To see the results of one month ionogram observations, the results of the daily LUF, MUF and OWF calculations will be recalculated to get the monthly median results. The monthly LUF, MUF and OWF median values will be calculated to get the annual median results which

are used as annual observation data. The results of the ionogram data processing will determine the channel openness as well as the frequency change graph that can be used from 2010 to 2015. Figure 5 shows a graph of the LUF, OWF and MUF values in 2010 which represent the minimum phase of the solar cycle.

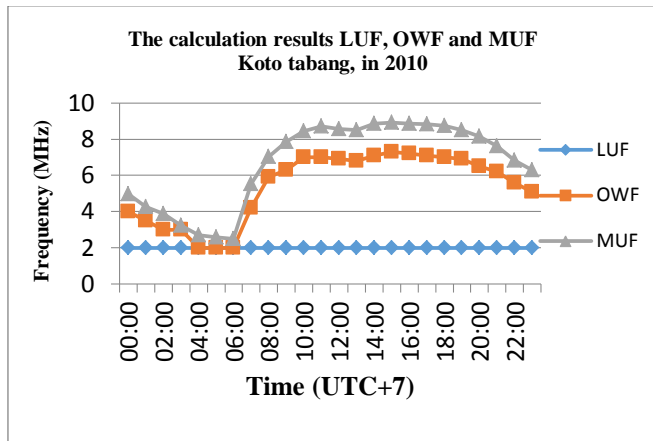


Fig. 5. Graph of the calculation results *LUF*, *OWF* and *MUF* in 2010

In the picture above, it can be seen that the lowest frequency (*LUF*) in 2010 was at a frequency of 2 MHz and the highest frequency value (*MUF*) varied over time. The peak of the *MUF* value occurred at 15.00 UTC+7 which was at a frequency of 8.9 MHz. This change is due to the fact that during the day the ionosphere layer gets more x-rays and extreme ultra-violet rays, which are more in the F ionosphere layer. Meanwhile, at 06.00 UTC+7 the *MUF* value decreased significantly at the frequency of 3.6 MHz. This is because at night until the early morning the number of electrons in the ionosphere layer becomes less caused by a decrease in the emission of x-rays and extreme ultra violet rays from the ionosphere layer.

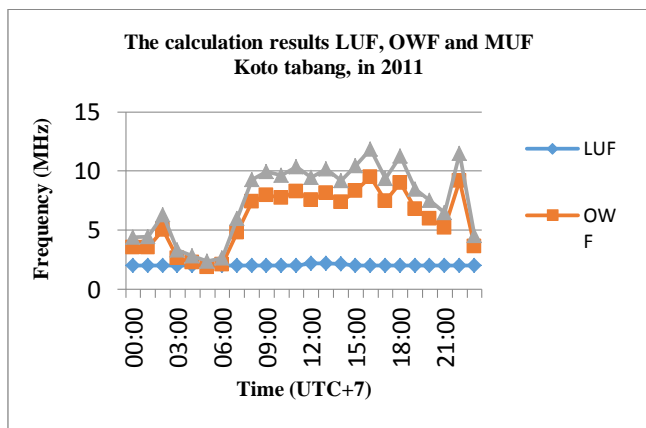


Fig. 6. Graph of the calculation results *LUF*, *OWF* and *MUF* in 2011

In the picture above, it can be seen that the lowest frequency (*LUF*) in 2011 was at a frequency of 2 MHz and the highest frequency value (*MUF*) varied over time. The peak value of *MUF* occurs at 09.00 UTC+7 which is at a frequency of 11 MHz. This change is due to the fact that during the day the ionosphere layer gets more x-rays and extreme ultra-violet rays, which are more in the F ionosphere layer. Meanwhile, at 05.00 UTC+7 the *MUF* value decreased significantly at the frequency of 3.1 MHz.

value decreased significantly at the frequency of 2.3 MHz. This is because at night until the early hours of the morning the number of electrons in the ionosphere layer becomes less due to a decrease in the emission of x-rays and extreme ultra violet rays from the ionosphere layer.

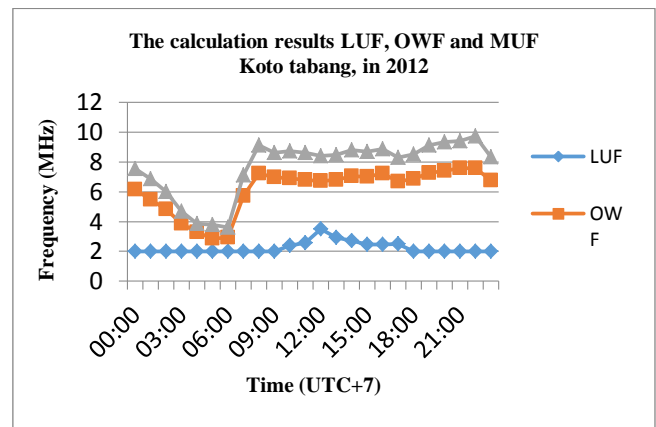


Fig. 7. Graph of the calculation results *LUF*, *OWF* and *MUF* in 2012

In the picture above, it can be seen that the lowest frequency (*LUF*) in 2012 was at a frequency of 2 MHz and the highest frequency value (*MUF*) varied over time. The peak of the *MUF* value occurred at 16.00 UTC+7 which was at a frequency of 9.7 MHz. This change is due to the fact that during the day the ionosphere layer gets more x-rays and extreme ultra-violet rays, which are more in the F ionosphere layer. Meanwhile, at 06.00 UTC+7 the *MUF* value decreased significantly at the frequency of 3.6 MHz. This is because at night until the early hours of the morning the number of electrons in the ionosphere layer becomes less due to a decrease in the emission of x-rays and extreme ultra violet rays from the ionosphere layer.

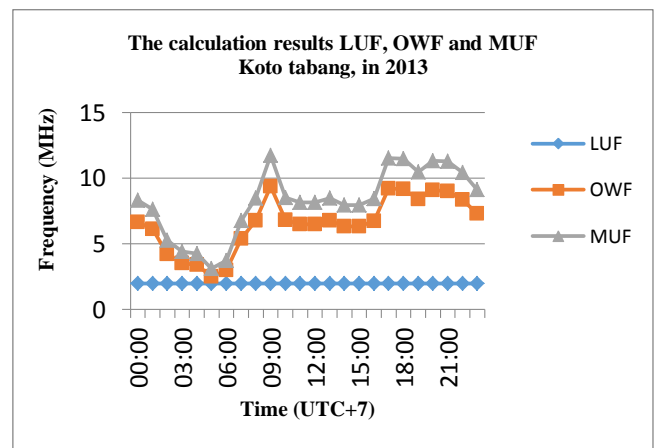


Fig. 8. Graph of the calculation results *LUF*, *OWF* and *MUF* in 2013

In the picture above, it can be seen that the lowest frequency (*LUF*) in 2013 was at a frequency of 2 MHz and the highest frequency value (*MUF*) varied over time. The peak value of *MUF* occurs at 09.00 UTC+7 which is at a frequency of 11 MHz. This change is due to the fact that during the day the ionosphere layer gets more x-rays and extreme ultra-violet rays, which are more in the F ionosphere layer. Meanwhile, at 05.00 UTC+7 the *MUF* value decreased significantly at the frequency of 3.1 MHz.

This is because at night until the early hours of the morning the number of electrons in the ionosphere layer becomes less due to a decrease in the emission of x-rays and extreme ultra violet rays from the ionosphere layer.

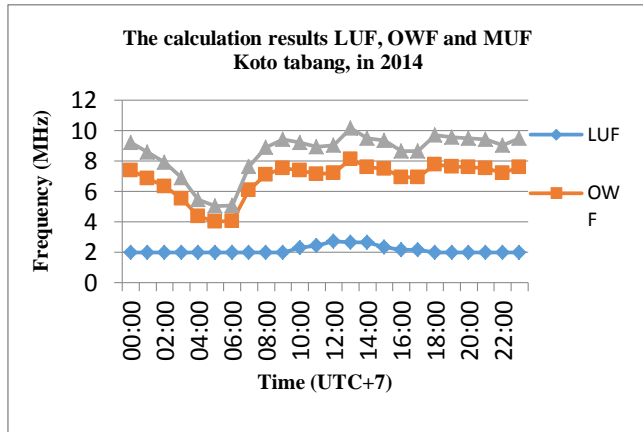


Fig. 9. Graph of the calculation results *LUF*, *OWF* and *MUF* in 2014

In the picture above, it can be seen that the lowest frequency (*LUF*) in 2014 was at a frequency of 2 MHz and the highest frequency value (*MUF*) varied over time. The peak value of *MUF* occurs at 13.00 UTC+7 which is at a frequency of 10 MHz. This change is due to the fact that during the day the ionosphere layer gets more x-rays and extreme ultra-violet rays, which are more in the F ionosphere layer. Meanwhile, at 05.00 UTC+7 to 06.00 WIB, the *MUF* value decreased significantly at the 5.0 MHz frequency. This is because at night until the early hours of the morning the number of electrons in the ionosphere layer becomes less due to a decrease in the emission of x-rays and extreme ultra violet rays from the ionosphere layer.

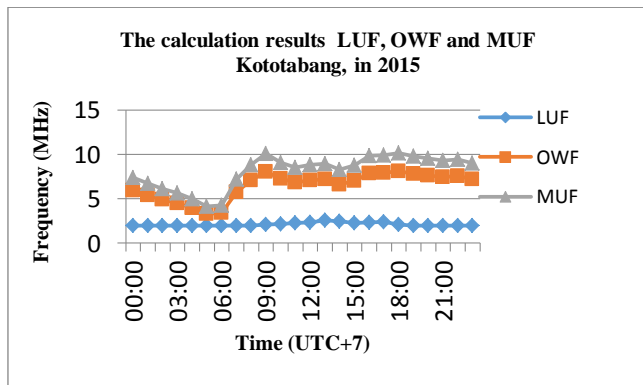


Fig. 10. Graph of the calculation results *LUF*, *OWF* and *MUF* in 2015

In the picture above, it can be seen that the lowest frequency (*LUF*) in 2014 was at a frequency of 2 MHz and the highest frequency value (*MUF*) varied over time. The peak of the *MUF* value occurred at 09.00 UTC + 7 which was at a frequency of 10 MHz. This change is due to the fact that during the day the ionosphere layer gets more x-rays and extreme ultra-violet rays, which are more in the F ionosphere layer. Meanwhile, at 05.00 UTC+7 the *MUF* value decreased significantly at the 4.1 MHz frequency. This is because at night until the early morning the number of electrons in the ionosphere layer becomes less caused by

a decrease in the emission of x-rays and extreme ultra violet rays from the ionosphere layer.

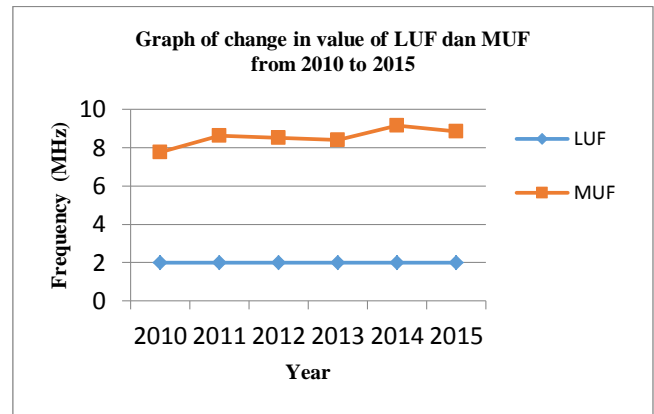


Fig. 11. Graph of Changes in *LUF* and *MUF* Values from 2010 to 2015

Figure 11 shows a graph of changes in the frequency of *LUF* and *MUF* from 2010 to 2015 which represents a half cycle of solar activity. Based on the graph, it can be analyzed that the *LUF* frequency from 2010 to 2015 did not change and tended to be stable at 2 MHz because the minimum frequency in layer E did not experience a high enough ionization process. The year 2010 is the initial phase of solar activity and tends to be in a calm condition because changes that occur in the Earth's magnetosphere have a significant contribution to the structure and dynamics of the ionosphere. Changes in the *MUF* value experienced a significant increase in 2010 to 2011 and 2013 to 2014 due to the increase in geomagnetic activity, plasma density and electric field in the low latitude ionosphere layer. Changes in the *MUF* value which decreased from 2011 to 2012, 2012 to 2013 and 2014 to 2015 were caused by negative storms that occurred in the ionosphere layer. This negative storm will cause a negative effect by changing the density of the ionosphere due to the transportation process. Negative storms are caused by changing the composition of the atmosphere due to reduced ionized plasma.

IV. CONCLUSION

Based on the research that has been done by Data analysis of *Near Vertical Incidence Skywave (NVIS)* Propagation In Pekanbaru, it can be concluded as follows:

1. The effect of solar activity on the ionosphere layer in the Pekanbaru area can affect the openness of the HF radio channel as evidenced by the difference in the use of working frequency every year,
2. The working frequency that can be used in 2010 is 2 MHz to 9 MHz, with the dominant frequency being 7 MHz. In 2011 the working frequency that can be used is 2.1 to 9.1 MHz, with the dominant frequency being 8 MHz.
3. The working frequency that can be used in 2012 the working frequency that can be used is 2 to 9 MHz, with the dominant frequency being 6.7 MHz. while in 2013 the working frequency that can be used is 2 to 10 MHz, with a dominant frequency of 6 MHz.
4. In 2014 the working frequency that can be used is 3 to 8 MHz, with a dominant frequency of 7 MHz. In 2015 the

working frequency that can be used is 2 to 10 MHz, with a dominant frequency of 7 MHz.

5. The lowest usable frequency (LUF) in the half cycle is at a frequency of 2 MHz and tends to be stable because the minimum frequency in layer E does not experience a high enough ionization process.
6. The value of the maximum usable frequency (MUF) experiences variations, changes in frequency tend to increase due to positive storms and changes in frequency decrease due to negative storms that occur in the ionosphere layer.

REFERENCES

- [1] S. Perhirin and Y. Auffret, "A low consumption electronic system developed for a 10km long all-optical extension dedicated to sea floor observatories using power-over-fiber technology and SPI protocol," *Microw. Opt. Technol. Lett.*, vol. 55, no. 11, pp. 2562–2568, 2013, doi: 10.1002/mop.
- [2] D. Irawan, T. Saktioto, Iwantono, Minarni, Juandi, and J. Ali, "An optimum design of fused silica directional fiber coupler," *Optik (Stuttg.)*, vol. 126, no. 6, pp. 640–644, 2015, doi: 10.1016/j.ijleo.2015.01.031.
- [3] D. Irawan, . Saktioto, and J. Ali, "Linear and triangle order of NX3 optical directional couplers: variation coupling coefficient," *Photonic Fiber Cryst. Devices Adv. Mater. Innov. Device Appl. IV*, vol. 7781, p. 77810J, 2010, doi: 10.1117/12.862573.
- [4] T. Purnamirza *et al.*, "Cutting Technique for Constructing Small Radial Line Slot Array Antennas," *J. Electromagn. Eng. Sci.*, vol. 21, no. 1, pp. 35–43, 2021, doi: 10.26866/jees.2021.21.1.35.
- [5] Yuda Irawan, A. W. Novrianto, and H. Sallam, "Cigarette Smoke Detection And Cleaner Based On Internet Of Things (IoT) Using Arduino Microcontroller And MQ-2 Sensor," *J. Appl. Eng. Technol. Sci.*, vol. 2, no. 2, pp. 85–93, 2021, doi: 10.37385/jaets.v2i2.218.
- [6] N. Rahayu and A. T. Sumarni, "Goods Robots Based On Color Using Microcontroller Atmega 328," *J. Appl. Eng. Technol. Sci.*, vol. 2, no. 2, pp. 50–61, 2021, doi: 10.37385/jaets.v2i1.144.
- [7] O. Kodheli *et al.*, "Satellite Communications in the New Space Era: A Survey and Future Challenges," *IEEE Commun. Surv. Tutorials*, vol. 23, no. 1, pp. 70–109, 2021, doi: 10.1109/COMST.2020.3028247.
- [8] T. Purnamirza *et al.*, "A design of radial line slot array antennas using the specification of panel antennas," *Telkomnika (Telecommunication Comput. Electron. Control.)*, vol. 17, no. 6, 2019, doi: 10.12928/TELKOMNIKA.v17i6.12679.
- [9] M. L. Hamzah, Y. Desnelita, A. A. Purwati, E. Rusilawati, R. Kasman, and F. Rizal, "A review of Near Field Communication technology in several areas," *Espacios*, vol. 40, no. 32, 2019.
- [10] M. L. Hamzah, Ambiyar, F. Rizal, W. Simatupang, D. Irfan, and Refdinal, "Development of Augmented Reality Application for Learning Computer Network Device," *Int. J. Interact. Mob. Technol.*, vol. 15, no. 12, pp. 47–64, 2021, doi: 10.3991/ijim.v15i12.21993.
- [11] Y. Irawan, R. Wahyuni, M. Muhardi, H. Fonda, M. L. Hamzah, and R. Muzawi, "Real Time System Monitoring and Analysis-Based Internet of Things (IoT) Technology in Measuring Outdoor Air Quality," *Int. J. Interact. Mob. Technol.*, vol. 15, no. 10, pp. 224–240, 2021, doi: 10.3991/ijim.v15i10.20707.
- [12] V. H. Cid, A. R. Mitz, and S. J. Arnesen, "Keeping Communications Flowing during Large-scale Disasters: Leveraging Amateur Radio Innovations for Disaster Medicine," *Disaster Med. Public Health Prep.*, vol. 12, no. 2, pp. 257–264, 2018, doi: 10.1017/dmp.2017.62.
- [13] R. C. Coile, "The role of amateur radio in providing emergency electronic communication for disaster management," *Disaster Prev. Manag. An Int. J.*, vol. 6, no. 3, pp. 176–185, 1997, doi: 10.1108/09653569710172946.
- [14] L. Edwards, "The utilization of amateur radio in disaster communications," *FHMI Publ.*, p. 59, 1994, [Online]. Available: http://https://scholarcommons.usf.edu/fmhi_pub/59.
- [15] W. Li *et al.*, "Joint Channel Selection and Data Scheduling in HF Jamming Environment: An Interference-Aware Reinforcement Learning Approach," *IEEE Access*, vol. 7, pp. 157072–157084, 2019, doi: 10.1109/ACCESS.2019.2948935.
- [16] K. Xu *et al.*, "+ LJK) UHTXHQF \ & RPPXQLFDWLRQ 1HWZRUN ZLWK ' LYHUVLW \ 6 \ VWHP 6WUXFWXUH DQG . H \ (QDEOLLQJ," pp. 46–59, 2018.
- [17] S. D. Abdullah, A. Arief, and M. Muhammad, "Utilization of NVIS HF Radio As Alternative Technologies In Rural Area of North Maluku," vol. 1, no. Icst, pp. 734–739, 2018, doi: 10.2991/icst-18.2018.149.
- [18] U. Umaisaroh, G. Hendrantoro, A. Mauludiyanto, and T. Fukusako, "Capacity of 2 2 MIMO HF NVIS Channels with Linearly Polarized Horizontal Antennas," *IEEE Wirel. Commun. Lett.*, vol. 8, no. 4, pp. 1120–1123, 2019, doi: 10.1109/LWC.2019.2908648.
- [19] B. A. Witvliet, R. M. Alsina-Pagès, E. Van Maanen, and G. J. Laanstra, "Design and validation of probes and sensors for the characterization of magneto-ionic radio wave propagation on near vertical incidence skywave paths," *Sensors (Switzerland)*, vol. 19, no. 11, 2019, doi: 10.3390/s19112616.
- [20] B. A. Witvliet and R. M. Alsina-Pagès, "Erratum to: Radio communication via Near Vertical Incidence Skywave propagation: an overview (Telecommunication Systems, (2017), 66, 2, (295-309), 10.1007/s11235-017-0287-2)," *Telecommun. Syst.*, vol. 66, no. 4, p. 713, 2017, doi: 10.1007/s11235-017-0319-y.
- [21] B. A. Witvliet and R. M. Alsina-Pagès, "Radio communication via Near Vertical Incidence Skywave propagation: an overview," *Telecommun. Syst.*, vol. 66, no. 2, pp. 295–309, 2017, doi: 10.1007/s11235-017-0287-2.
- [22] L. . McNamara, *The Ionosphere: Communications, Surveillance, and Direction Finding*. Krieger Publishing Company, 1991.
- [23] Z. Wu, H. Chen, Y. Lei, and H. Xiong, "Recognizing automatic link establishment behaviors of a short-wave radio station by an improved unidimensional densenet," *IEEE Access*, vol. 8, pp. 96055–96064, 2020, doi: 10.1109/ACCESS.2020.2997380.
- [24] Sutoyo, "Utilization of Measurement Data of Ionosphere Observation Station for Continuation of Radio HF Channel Information," in *2018 Electrical Power, Electronics, Communications, Controls and Informatics Seminar, EECCIS 2018*, 2018, doi: 10.1109/EECCIS.2018.8692875.
- [25] L. A. A. Guzmán, E. M. Ovalle, and R. A. Reeves, "Measurement of the Ionospheric Reflection Height of an HF Wave in Vertical Incidence With a Resolution of Minutes," *IEEE Geosci. Remote Sens. Lett.*, vol. 15, no. 11, pp. 1637–1641, 2018, doi: 10.1109/LGRS.2018.2856110.
- [26] V. Dear, A. Husin, S. Anggarani, J. Harjosuwito, and R. Pradipta, "Ionospheric Effects During the Total Solar Eclipse Over Southeast Asia-Pacific on 9 March 2016: Part 1. Vertical Movement of Plasma Layer and Reduction in Electron Plasma Density," *J. Geophys. Res. Sp. Phys.*, vol. 125, no. 5, pp. 1–40, 2020, doi: 10.1029/2019JA026708.